Not available on line

Not available on line

Not available on line

Not available on line

Not available on line

Not available on line

Not available on line

Not available on line

Not available on line

Not available on line

CEFDA04-1138

Task Title: TW4-TVB-HFCSMU: HIGH HEAT FLUX TESTING OF OPTIMISED CuCrZr/SS MOCK-UPS 200 KW ELECTRON BEAM GUN TEST

INTRODUCTION

Thermomechanical fatigue is one of the most important damaging mechanisms for the plasma facing components (PFC) of the ITER machine due to the high number of operating cycles (several thousands) and to the expected surface heat loads. Therefore an assessment of the behaviour of PFC under cycling heat loads is essential to demonstrate the fitness for purpose f the selected design solutions. This contract concerns the monitoring and analysis of thermal fatigue testing of PFC to be performed in the frame of the European R&D programme for ITER.

In the frame of this, three mock-ups were thermal fatigue tested at FE200 [1] in 2005:
- CuCrZr/SS first wall mock-ups (mock-up FW8)
- W armoured monoblocks (mock-up VTFS)
- CFC armoured monoblocks (mock-up Baffle B,C)

The activities planned in the frame of this contract are now completed.

2005 ACTIVITIES

MAIN RESULTS

CuCrZr/SS first wall mock-ups (mock-up FW8)

A manufacturing route for the production of Primary First Wall Panels (PFW) involves a high temperature HIPing at 1040°C for joining the CuCrZr alloy heat sink materials to the 316L Stainless Steel (SS) back plate. Beryllium (Be) armour is then joined by HIPing at a temperature range of 560-580°C. In order to allow the retention of sufficient mechanical strength with the CuCrZr, two alternative routes are being considered: high temperature HIP quenching, i.e. HIP cycle with fast cooling within the HIP furnace, followed by an ageing heat treatment or a high temperature HIP cycle with a subsequent solution annealing heat treatment with fast cooling also followed by an ageing heat treatment. In comparison with the prime aged heat treatment, all the above heat treatment cycle slightly degrade the tensile strength of the CuCrZr alloy. Two elements without beryllium were manufactured following the above alternative routes (PH/S-8F and PH/S-9F) and tested at FE200 to compare their fatigue behaviour. These two elements are made of a 20 mm thick CuCrZr heat sink HIPed onto a 30 mm thick Stainless Steel back plate; 4 Stainless Steel cooling tubes of outer diameter 12 mm, thickness 1 mm, are inserted in between the two CuCrZr half-shells. The cooling tubes are welded to inlet and outlet manifolds for connection to water supply system, allowing the parallel flowing of the 2 elements. Dimensions of each element are 250 mm x 88 mm x 50 mm (figure 1).

a)

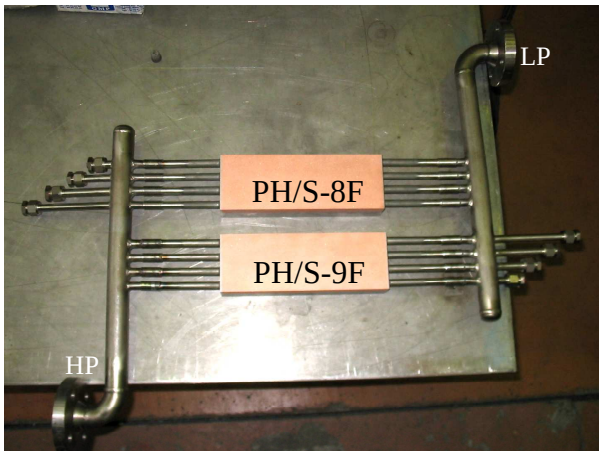

b)

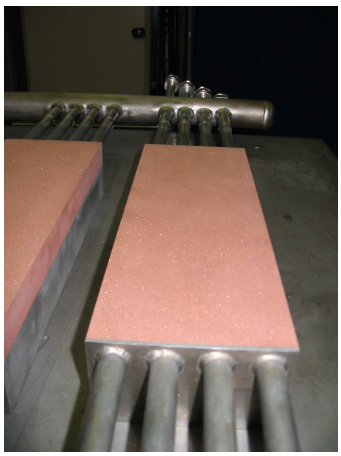

Figure 1: a) View of the mock-up FW8 = PH/S-8F + PH/S-9F, b) the CuCrZr was sandblasted before testing to increase infra-red emissivity

The cooling water conditions for the tests were selected at inlet temperature 100°C, flow rate 3 kg/s (i.e. 4.8 m/s), inlet pressure 3.3 MPa (ITER first wall relevant conditions), dimensions of the heated area 160 mm x 88 mm.
Both of the elements resisted successfully a first step of fatigue 1000 cycles at 5 MW/m² 15 sec. ON / 15 sec. OFF: no obvious observation of surface temperature was observed during this step.

During the second step of fatigue at 7 MW/m², a defect propagation was detected onto the element PH/S 9F after 143 cycles, the fatigue step was interrupted on this mock-up and continued on PH/S-8F up to the 267th cycles when indication of defect propagation was also detected (figure 2).

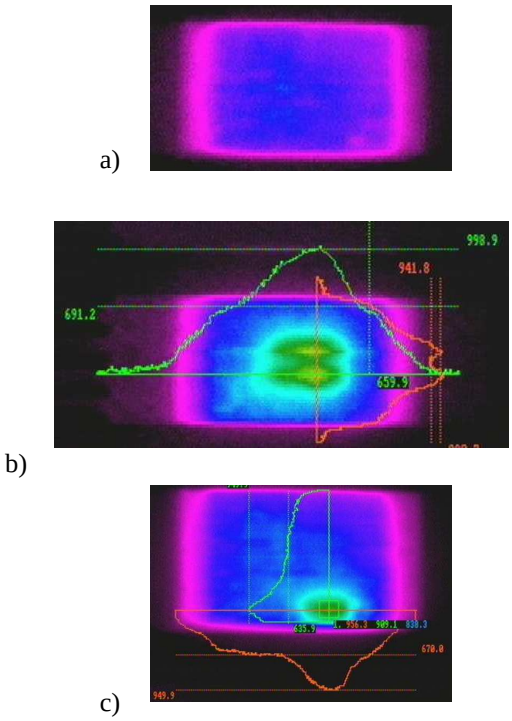

Figure 2: Infrared detection of defect propagation
a) Standard infrared pattern
b) Defect propagation on PH/S-9F after 143 cycles
c) Defect propagation on PH/S 8F after 267 cycles

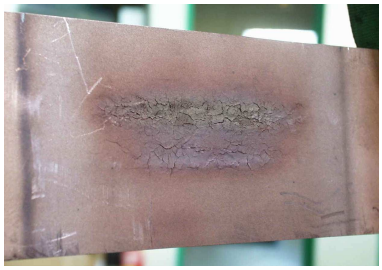

Figure 3: Zoom on PH/S-9F surface with clear correlation between CuCrZr surface state (intergranular cracks at the burned boundary grains Copper) and infrared temperature evaluation (~1000°C)

Conclusion on FW8 Testing:

Post-testing metallographic analysis will be performed by the manufacturer to optimize allow the manufacturing route.

Warmoured monoblocks (mock-up VTFS)

The Vertical Target Full Scale mock-up manufactured by PLANSEE was already extensively tested in the frame of the contract CEFDA 01-585: successful fatigue steps of 1000 cycles at 20 and 23 MW/m² absorbed confirmed the robustness of the CFC monoblock whereas a limit at 10 MW/m² was found for the W monoblocks with systematic occurrence of water leaks during fatigue cycling [2].
A third and last testing campaign was performed at FE200 in 2005 in the frame of this task. Transversal castellations were machined every 20 mm on the W armoured monoblocks in order to decrease the thermomechanical stress due to thermal expansion during the cycling into the block and at the interfaces W/pure Copper/CuCrZr.

A successful cycling step of 1000 cycles at 20 MW/m² absorbed was performed without degradation of the W monoblocks on a area which was not fatigued before the machining of castellation (figure 4).

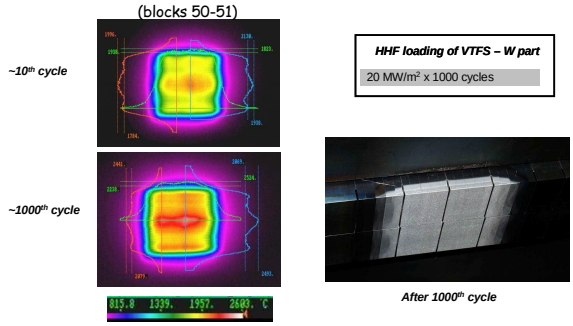

Figure 4: Main results on W monoblocks of the mock-up VTFS

Conclusion on VTFS Testing:

The transversal castellation of W monoblocks is mandatory and will be required in all future components for the ITER Divertor designed to endure more than 10 MW/m².

CFC armoured monoblocks (mock-up Baffle B, C)

The Baffle B, C mock-up manufactured by FRAMATOME in Partnership with PLANSEE was already tested in the frame of the contract CEFDA01-585 [3]: 2 kinds of geometries were manufactured (figure 5) and successfully fatigue tested during steps of 1000 cycles at 10 MW/m². Note that due to the curvature radius of the baffle, the axial dimension of a monoblock is reduced down to 4 mm instead of standard 20 mm in case of Divertor straight targets application.

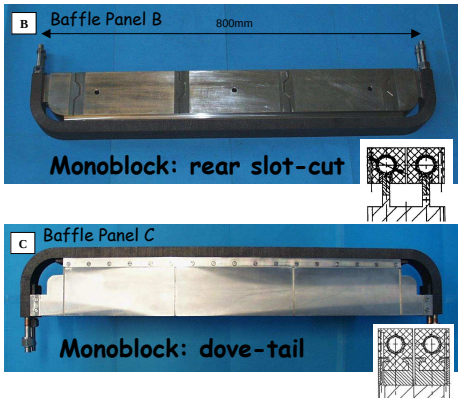

Figure 5: Panel B with slot-cut attachment and Panel C with dove-tail attachment

A second and last testing campaign was performed at FE200 in 2005 in the frame of this task. It was decided to fatigue the CFC monoblocks with a heat flux of 16 MW/m² being a compromise between the nominal value (20 MW/m²) and the operational values at FE200 (Tsurf < 2000°C, no swirl = risk of Critical heat Flux)

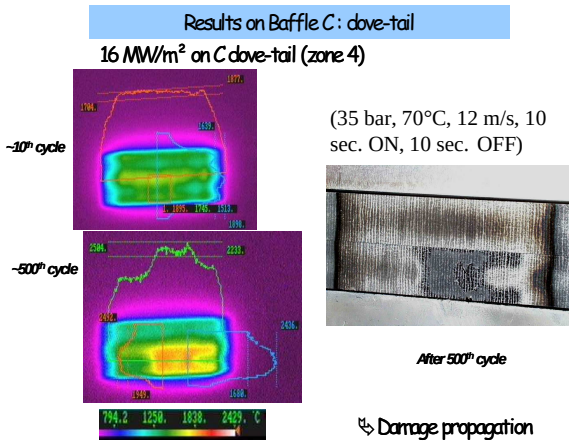

Figure 6: Observation of damage propagation

Cycling at 16 MW/m² on the slot-cut geometry was not possible due to the presence of micro water leaks (vacuum degradation from 10^{-4} to 10^{-3}-10^{-2} mb) probably due to the presence of fatigue cracks into the CuCrZr tube appeared during the cycling at 10 MW/m², a future metallographic examination would confirm this assumption.

On the dove-tail geometry, 4 zones of 140 x 50 mm, which means 280 blocks, were cycled. No perturbation was observed on zoes 1; 2 and 3 and one damage propagation after 500 cycles was clearly observed on zone 4.
Figure 6: Observation of damage propagation
A study on SATIR non-destructive examination and first screening at FE200 allows the initial dimensions of the defect to be determined: location at 45° from the top of the tube, extension 140°. The final screening at FE200 shows an axial propagation (from 1 block to 4 blocks) and also a circumferential propagation > 140° (figure 7).

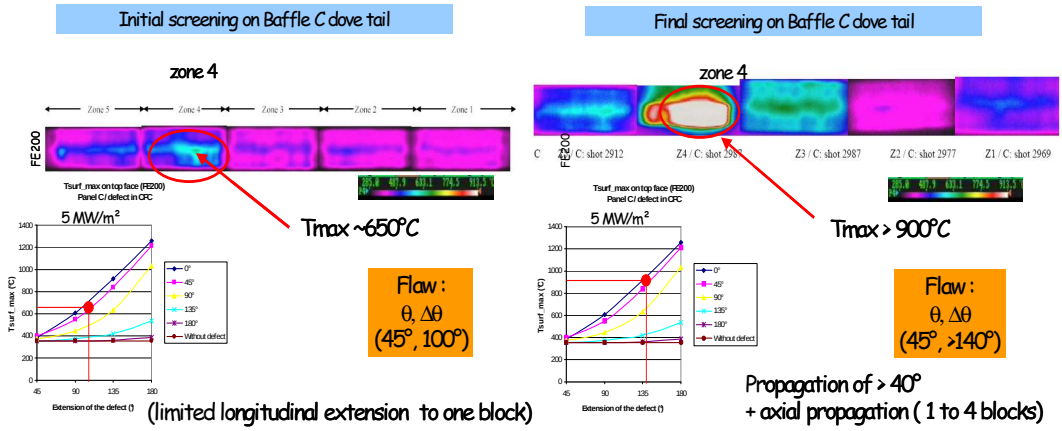

Figure 7: Evaluation of damage propagation

CONCLUSIONS

SLOT-CUT GEOMETRY

The fact that the sliding due to the thermal expansion of CFC under heat flux is not allowed by the rear slot -cut technology seems to be a weak point during thermal cycling. This geometry is not relevant for a PFC designed for 20 MW/m².

DOVE-TAIL GEOMETRY

280 blocks with dove-tail geometry sustained 1000 cycles at 16 MW/m², however a defect propagation was observed and assessed, a future metallographic examination would confirm this evaluation.

REFERENCES

[1] Fus. Eng. Des. 75-79 (2005) 357-363, I. Bobin-Vastra, F.Escourbiac, M.Merola et al.
[2] Fus. Eng. Des. 75-79 (2005) 435-440, M.Missirlian, F.Escourbiac, M.Merola et al.
[3] Contract EFDA 01/585 - Final Report, CFP/NTT-2005.008, F.Escourbiac, 2005

TASK LEADER

Frédéric ESCOURBIAC

DSM/DRFC/SIPP
CEA-Cadarache
F-13108 Saint-Paul-lez-Durance Cedex

Tel. : 33 4 42 25 44 00
Fax. : 33 4 42 25 49 90

e-mail : frederic.escourbiac@cea.fr

CEFDA04-1218

Task Title: TW5-TVD-HHFT: MONITORING AND ANALYSIS OF DIVERTOR COMPONENTS TESTED IN FE200 200 KW ELECTRON BEAM GUN TEST

INTRODUCTION

Thermal fatigue is one of the most important damaging mechanisms for the Plasma Facing Components (PFCs) of the ITER machine due to its high number of operating cycles (several thousands) and to the expected surface heat loads. Therefore an assessment of the behaviour of PFCs under cycling heat loads is essential to demonstrate the fitness for purpose of the selected design solutions.
This Task concerns the thermal fatigue testing of plasma facing components to be performed in the frame of the European R&D programme for ITER.
The thermal fatigue testing forming the subject matter of the present activities are performed in FE200 electron beam facility at Le Creusot, France. This facility has been designed and built to properly simulate the high heat fluxes expected on the PFCs and it has performed tests for NET/EFDA since 1989 [1].

2005 ACTIVITIES

Two baffle full-scale panels manufactured by Framatome ANP in partnership with PLANSEE GmbH LECHBRUCK [2] were tested at FE200 in the frame of this task during the year 2005.

DESCRIPTION OF THE MOCK-UP

Each panel has two cooling channels, a typical length of about 800 mm and a width of 44 mm (cf. figures.1, 2 and 3) assembled on a Stainless steel support.

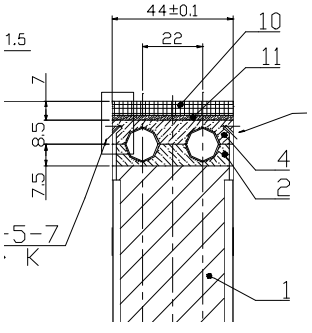

Figure 1: Transversal view of Baffle A-CFC panel

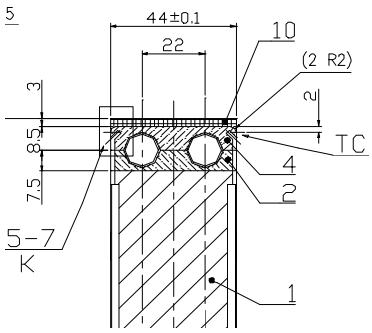

Figure 2: Transversal view of Baffle A-W panel

The heat sink is made of DS-Copper (CuAl25) including two 0.5mm thick stainless steel tubes. The S.S. support/CuAl25/S.S tube/CuAl25 assembly was realised by HIPing. The GBaffle A-CFC panel is armoured with 5 mm thick CFC NS31 tiles by AMC and Electron beam processes. The tiles dimensions are 19.2 mm long x 44 mm wide. On the flat part, there is a 1 mm gap between each of the 34 tiles. The Baffle A-W is armoured with a 3 mm thick (down to 0.1 mm on the lateral parts) Tungsten plasma-sprayed coating.

The two panels were equipped with 8 thermocouples and mounted on a cooled supporting system for connection to the FE200 pressurized water loop (figure 3), a dedicated Copper shield was sandwiched between the two panels, this mock-up was called “Baffles A-CFC/W”.

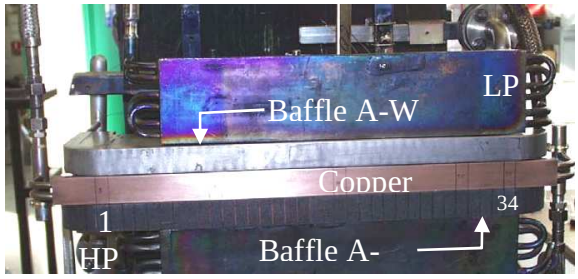

Figure 3: Mock-up “Baffles A-CFC/W”, view from the gun in the vacuum chamber at FE200High heat flux testing

HIGH HEAT FLUX TESTING

- Objective:

In order to check a capability for such technologies to withstand a few MW/m², the following test plan was performed [3]:

Table 1: Test plan at FE200

	Heat flux absorbed (MW/m²)	
	CFC panel	W panel
Screening	2.5	1.5
100 cycles at	2.5	1.5
1000 cycles at	3-3.5	2-2.5
1000 cycles at	5	3

The cooling water conditions at the inlet were 3.5 MPa, 10 m/s, 100°C, there is no twisted tape into the cooling channel, the duration of cycles is 10 sec. ON, 10 sec. OFF.

Figure 4: Definition of the heated zones

- Results [4]:

The following zones were defined for the tests:

The screening of the Baffle A-W panel was performed at an absorbed heat flux of 2.5 MW/m², discrepancies of evaluated surface temperature by the infrared devices are linked both to the coating thickness and emissivity (figure 5). In comparison, the infrared picture of the CFC is remarkably homogeneous at 300°C except some stable hot spots (figure 6). After increasing of the absorbed power, a study on the measured surface temperature showed that on the CFC armour, the measurements were consistent with Finite Element analysis and that on the W coating, the thermal conductivity was 15% of the bulk conductivity (a previous study in 2001 has shown 10% [5]), cf. figure 5.

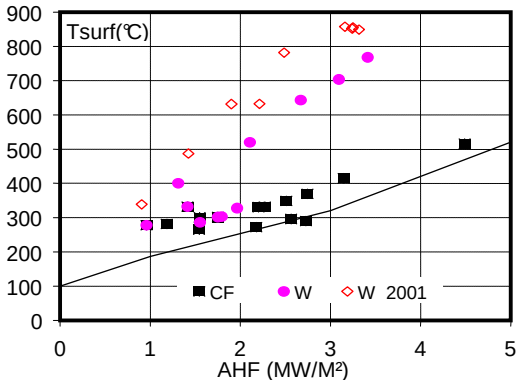

Figure 5: Surface temperature vs Absorbed Heat Flux

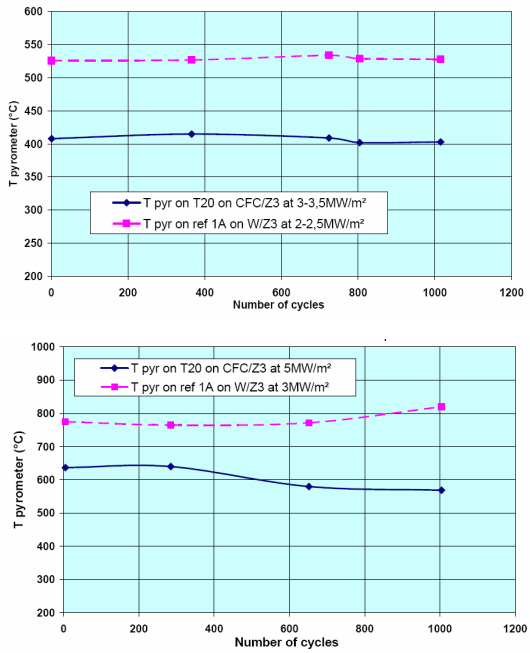

Figures 7 and 8: No evolution of surface temperature during cycling step: no degradation of the joint

No clear evolution of surface temperature was observed during the steps of cycling. The two steps of 1000 cycles are reported figures 7 and 8.

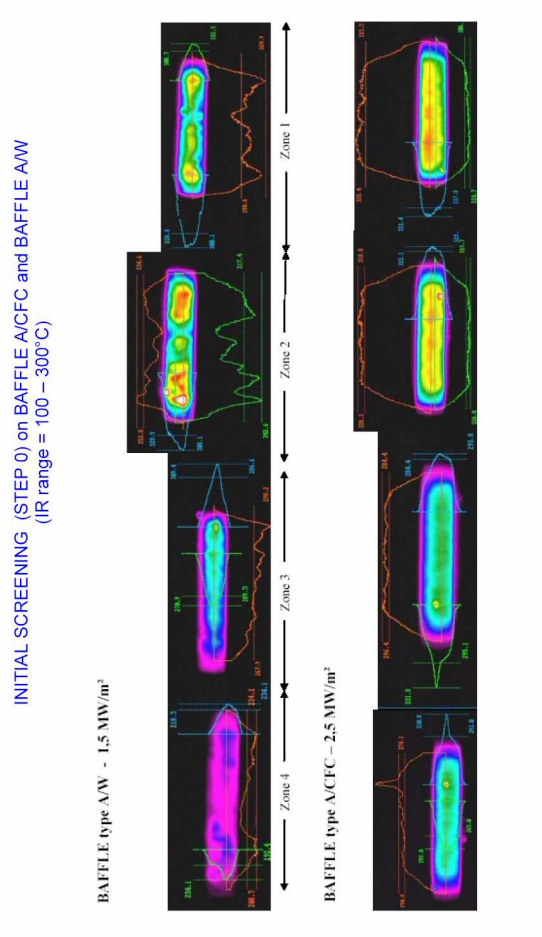

Figure 6: Infra red pictures of the screening

After the screening, the Zone 3 was identified for cycling steps.

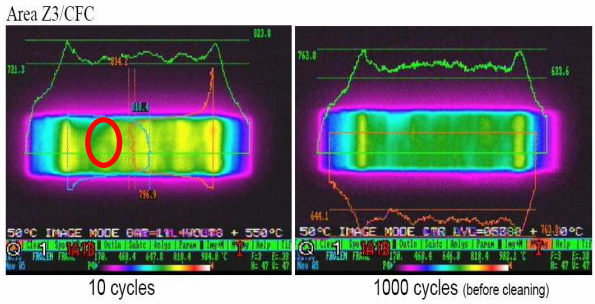

Figure.9: After 10 and 1000 cycles at 5 MW/m² absorbed on Baffle A-CFC – Red circle is for pyrometer position

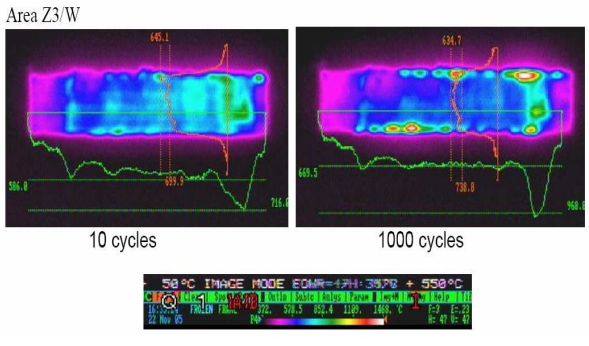

Figure.10: After 10 and 1000 cycles at 3 MW/m² absorbed on Baffle A-W

CONCLUSIONS

The stainless steel tubes embedded inside the 2 half blocks of Copper offer an efficient protection against water leaks even if the HIPed interface debonds, on another hand, the global heat transfer capability of the component is lowered by the presence of stainless steel, consequently, these baffles are not designed to withstand the divertor loads (up to 20 MW/m²) but can be foreseen in those plasma facing areas where a heat flux higher than that typical of the first wall panels is expected, say 3-5 MW/m² for respectively W and CFC armour (start-up limiter ?).

The activity will continue with 3 high heat flux campaigns on technologies for ITER divertor vertical target

REFERENCES

[1] Fus. Eng. Des. 75-79 (2005) 357-363, I. Bobin-Vastra, F.Escourbiac, M.Merola, P.Lorenzetto

[2] FRAMATOME-ANP report TFCW R 02. 883 A - – I.Bobin-Vastra, 09/12/02

[3] Spécifications techniques pour la maquette baffles A-CFC/W à tester au FE200 - CFP/NTT-2005.027 – F.Escourbiac, 2005

[4] AREVA report R-05.915A - NFTF - CEA87 – EFDA/93-851JN – I.Bobin-Vastra, 20/12/05

[5] Review of mock-up “Curved-WPS” FE200 testing - CFP/NTT-2001.028 – F.Escourbiac, 2001

TASK LEADER

Frédéric ESCOURBIAC

DSM/DRFC/SIPP
CEA-Cadarache
F-13108 Saint-Paul-lez-Durance Cedex

Tel. : 33 4 42 25 44 00
Fax : 33 4 42 25 49 90

e-mail : frederic.escourbiac@cea.fr

CEFDA05-1243

Task Title: TW5-TVD-NDTEST: UPGRADE OF THE SATIR TEST BED FOR INFRARED THERMOGRAPHIC INSPECTIONS

INTRODUCTION

Among all Non-Destructive Examinations, active infrared thermography by internal thermal excitation is becoming recognised as a technique available today for improving quality control of many materials and structures involved in heat transfer. The infrared thermography allows to characterize the brazing bond between two materials with different thermal physical properties. An infrared thermography test bed named SATIR (Station Acquisition Traitement InfraRouge) has been developed by CEA in order to evaluate the manufacturing process quality of actively water-cooled high heat flux components (PFC's) before their installation in Tore Supra. In order to increase the defect detection limit of the SATIR test bed, several possibilities have been assessed (CEFDA00-565). The installation in 2003 of a digital infrared camera and the improvement of the thermal signal processing, has led to a considerable increase of performances.

BACKGROUND

In 2001 the main conclusion of the following EFDA contract [1] named "Improvement evaluation for infrared detection of PFC flaws" showed that:

- The increasing of range temperature (up to 200°C) would involve complete pressurization of test bed. Finite element calculations showed that this solution allows a significant improvement of sensitivity (by factor 2) but it not retained because SATIR becomes less flexible in its use (Pressure Safety Standard).

- The implementation in 2003 of a cooled digital IR camera using wavelengths range 3-5µm instead of a scanning infrared camera allowed to develop a new data processing, which led to a significant improvement of performances.

- The increase of water velocity inside the tested component involves an increasing of the heat transfer convective coefficient, which improves in a significant way the sensitivity of SATIR diagnostic.

TEST BED DESCRIPTION

The principle of SATIR test (photo 1) is to generate successively a hot and a cold-water front in the cooling channel of the elements, in order to measure the surface temperature evolution.

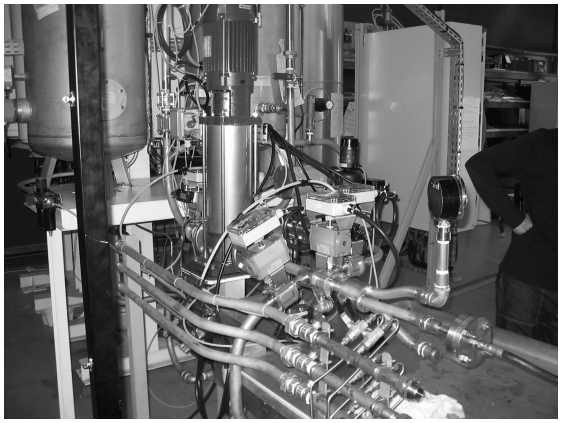

Photo 1: View of SATIR test bed

A cooled infrared digital camera is used to detect zones where heat exhaust is not sufficient. Defects like braze voids are detected by a slower temperature response on the surface during the transient. The geometry tolerances and the material property variations play a major role in the determination of acceptance criteria. In case of serie control, two components are tested in parallel to a reference. A DTref criterion is defined with respect to the reference. The detailed principle of SATIR facility and DTref Criterion were the subject of several publications [2].

JUSTIFICATION

Within the on-going work on acceptance criteria task, which is being carried out by EU and the ITER International team, SATIR inspection has been identified as the basis test to decide upon the final acceptance of the Divertor PFC's. However, the ITER Divertor PFC's pose new challenges for the following reasons:

- The CFC thickness is 2-3 times higher (18-20 mm) than any existing component manufactured or being manufactured so far either within the ITER project or within domestic projects. Therefore, the sensitivity of the technique, which depends on the armour thickness, is lowered.

- The number of units to be tested is 2-3 times higher (more than 2000) than on any existing or under construction fusion machine. Therefore, the total time required to test all the units increases accordingly.

This involves, as a consequence, the following needs:

i) To increase the water velocity

ii) To minimize the test time needed to check each component.

2005 ACTIVITIES

INCREASING OF WATER VELOCITY (I)

A simulation of SATIR experiment by finite element calculations (CAST3M, figure 1) has been carried out on ITER monobloc CFC following the conditions below:

- 2D modelling
- 2 testing lines in parallel (test and ref.)
- CFC_NB31 with thickness 5mm
- No linear model
- Cooling phase only
- Radiation exchange of the flaw
- Surface natural convection
- 3 flaw positions θ (0°, 45°, 90°) and 1 flaw extension Δθ (60°)

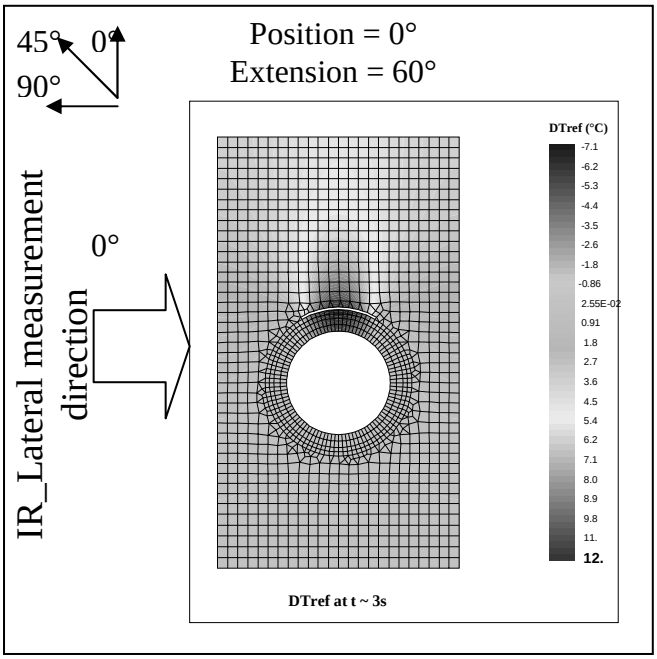

Figure 1: FE calculation θ=0°; Δθ=60°

The figure 2 illustrates the improvement of the DTref value versus the evolution of the SATIR water flow rate.
One can expect a significant increase of performances with a water flow enhancement:

- 55% for a flow rate of 10 m^3/h (12 m/s each elem.)
- 37% for a flow rate of 8 m^3/h (10 m/s each elem.)

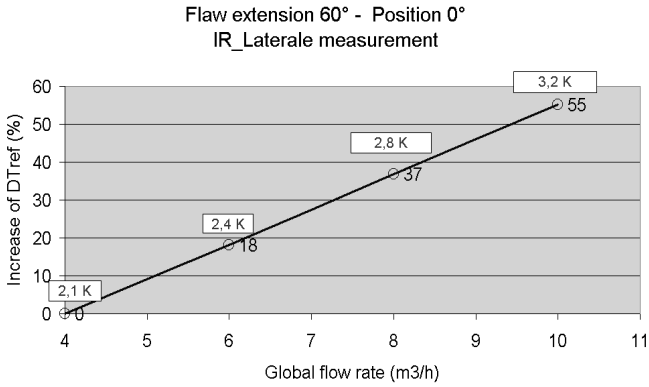

Figure 2: Flow rate effect on DTref

This assessment allowed to design an upgraded SATIR test bed taking into account the technical requirements of ITER mock-ups (table1). The new cold pump and the buffer tank will be implemented in 2006.

Table 1: Flow rate and pressure

Mocks-up parameters	ITER maximum requirements 2 // IVT
Q m^3/h	10 (12 m/s)
P bar	5

MINIMISE THE TEST TIME REQUIRED (ii)

The SATIR process will be significantly simplified using only two pulses. The envisaged solution will take into account only the cooling cycle instead of the two cycles usually used (figure 3).

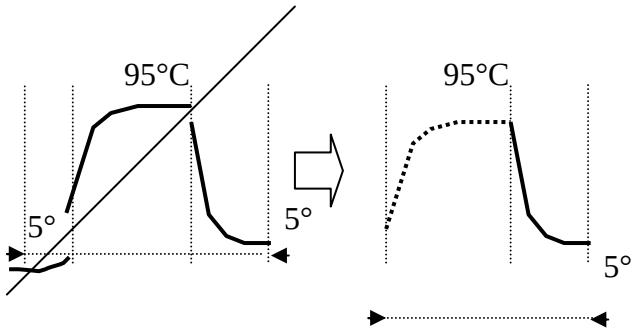

Figure 3: Solution! Only the cold water cycle

This issue will also involve an improvement of the detection sensitivity because the experience showed that the water dynamic viscosity was not the same between heating and cooling cycle. The heat transfer convective coefficient is higher at the beginning of the cooling phase. Furthermore this enhancement will allow:

- To reduce the film size (700 Mo to 300 Mo).
- To reduce the data process time by 2/3.
- To increase the reliability of pumps because it still works at the same temperature.
- To simplify the command control process.

PROPOSED IMPROVEMENT CONCEPT

SATIR was partially upgraded in 2005 by increasing the inlet pipe diameter and by improving the heating unit. SATIR upgrade Phase 2 is for compatibility with FULL SCALE DIVERTOR elements with a higher-pressure drop, based on new cold-water injection pump, buffer tank and feeding pumps to keep constant flow rate. (Appendix 1: Functional sketch and drawing).

2005: Phase 1 (preparation)
New heating unit: two adding hot tanks have been implemented (photo 2). The maximum heating time is two hours.
Heating units specifications: 0.3 m^3 each; heating time = 2 hours; Pe = 12 KW.
No modification of the cooling unit.
Scale inhibitor: To avoid the formation of scale inside the tanks and pipes.
Specifications: Q = 10 m^3/h; electromagnetic process.
Water network modification: To increase the diameter of water pipes and the flow rate capability.

2006: Phase 2 (construction)
New cold-water injection pump: to get a steepest slope on the thermo signal.
Pump specifications: 6 <Q< 10 m^3/h, 5 <P< 12 bar.
Hot water injection pump: no control of the by-pass will be implemented. The aim of this upgrade is to get rapidly the steady state temperature.
Pump specifications: 6 <Q< 8 m^3/h, 5 <P< 10 bar.
Buffer-tank: to keep a constant flow rate.
Buffer-tank specifications: 4 m^3; refilling time=18 mn.
Feeding pump: To feed both heating and cooling units and prevent them from depressurisation.

SCHEDULE AND COST OF THE EQUIPMENT

This phase 1 preparing has been anticipated in order to gain time to start the SATIR construction phase 2 earlier. The cost of the phase 1 reached 13875 euros. The next step phase 2 will reach 50000 euros (Appendix 2). The construction phase will last 10 weeks including piping, wiring, command control programming and debugging (Appendix 3).

Photo 2: View of the 2 adding heating tanks

CONCLUSIONS

In order to increase the defect detection sensitivity of the SATIR test bed, the possibility to improve the water velocity and to minimise the time required to test each component have been assessed. Finite element calculations showed an increase of 55% of DTref for a flow rate of 10 m^3/h. The main results are:

- Transition to next step at Q=10 m^3/h; (V=12m/s in each element) following the sketch shown in appendix.
- Only one cold water cycle to minimise the time required to test components.
- The cost of construction of the SATIR phase 2 reaches at 50 k€.
- 10 weeks of construction are required (week 27^{th} to 37^{th}, 2006) following the workplan showed in appendix 3.

REFERENCES

[1] "Improvement evaluation for infrared detection of PFC flaws" Final report CEFDA 00-565

[2] "Development of an original active thermography method adapted to ITER plasma facing components control" Fusion Engineering and Design 75-79 (2005) 401-405

TASK LEADER

Alain DUROCHER

DSM/DRFC/SIPP/GCFP
CEA-Cadarache
F-13108 Saint-Paul-lez-Durance Cedex

Tel. : 33 4 42 25 62 69
Fax : 33 4 42 25 49 90

e-mail : alain.durocher@cea.fr

APPENDIX 1

FUNCTIONAL SKETCH

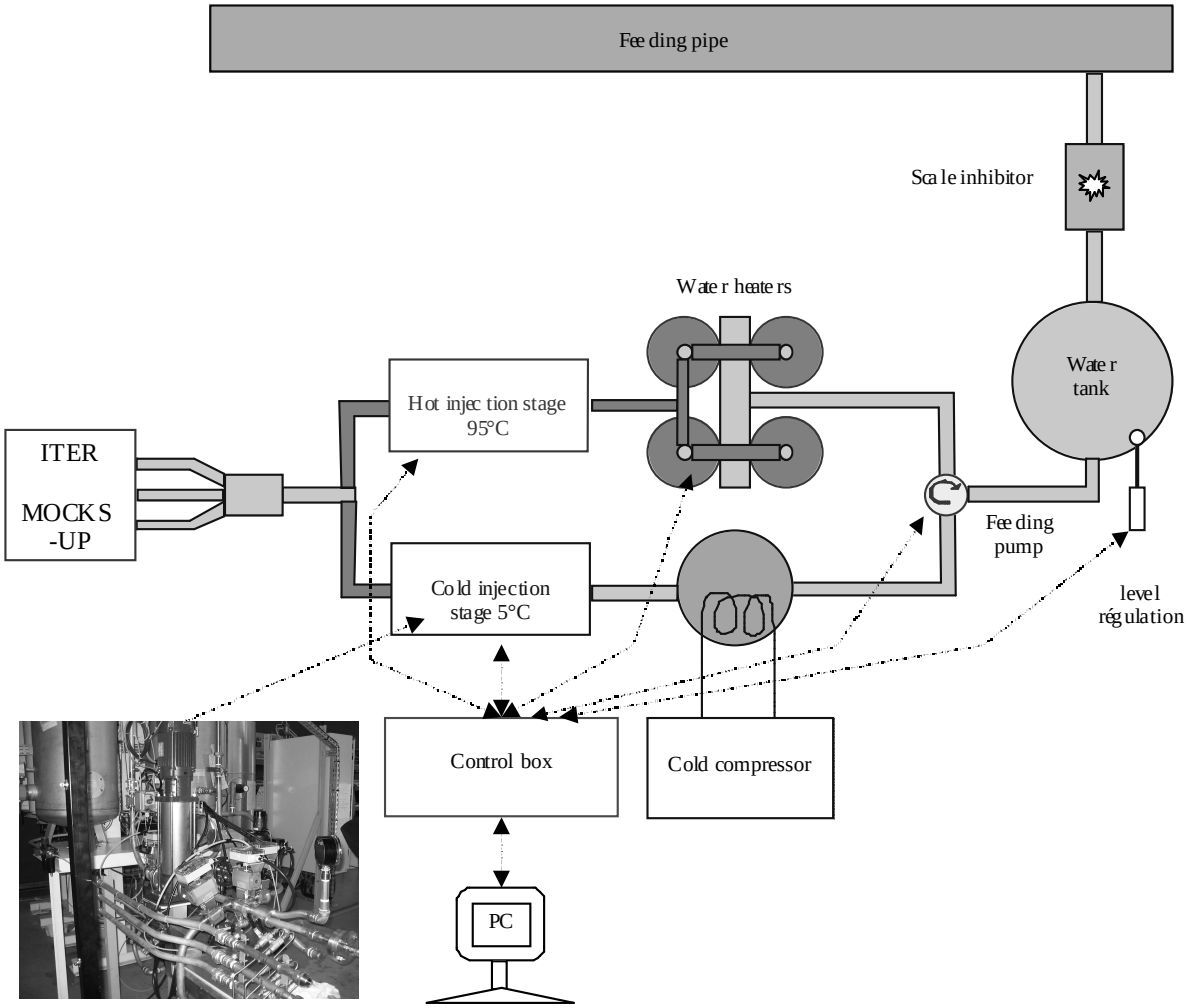

DRAWING

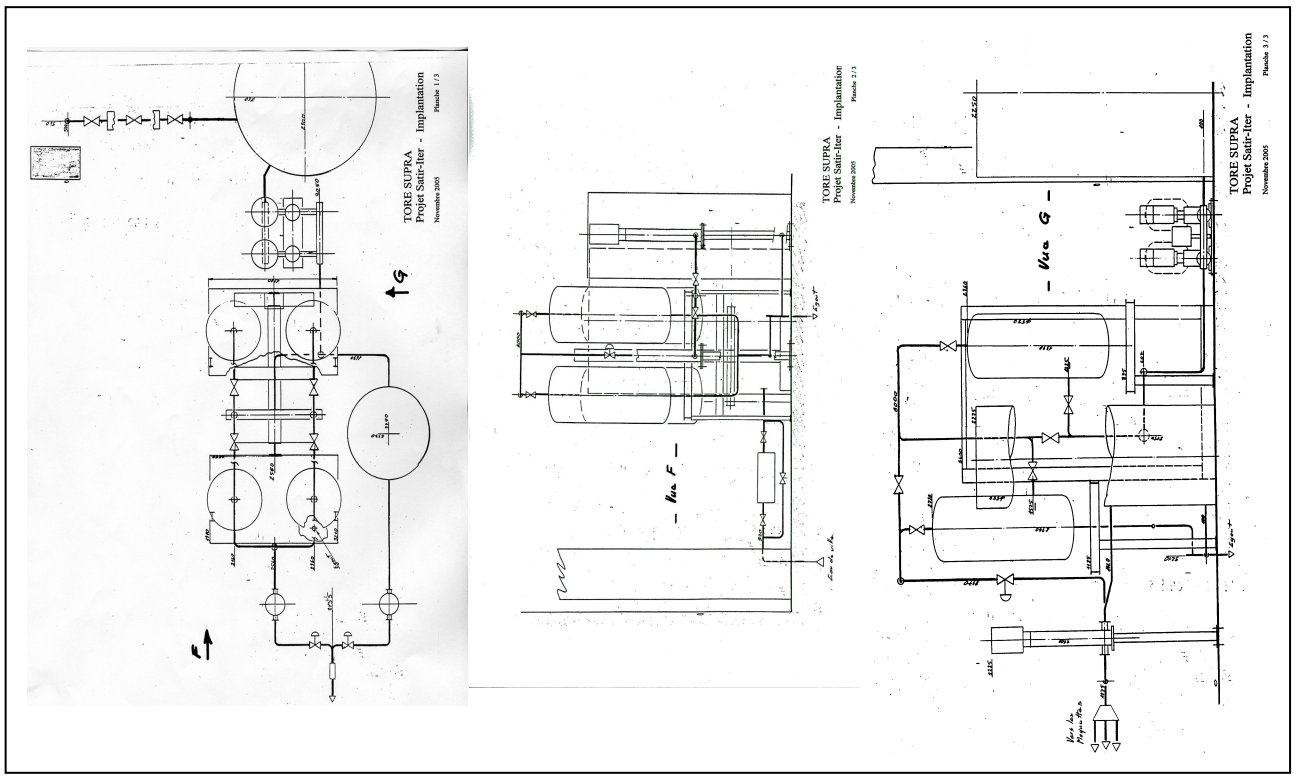

APPENDIX 2

COST OF EQUIPMENT

Nature of investments	2005	2006
Hydraulic tasks: -Water supply piping -New water heaters piping, Electric tasks: -Electrical power distribution	2570 9157 2148	
	total : **13875**	
Hydraulic tasks: -High pressure stages + Feeding pump -hydraulic items -Construction of the water buffer tank		2800 455 6500
		total : **9755**
Hydraulic items : -Valves, HP pump, feeding pump, water level regulation		17000
		total : **17000**
Electric tasks : -Command control box wiring -Electrical power distribution -Technical assistance for startup + settings -Data acquisition wiring		19000 4246
		total : **23246**
TOTAL	**13875 Euros**	**50000 Euros**

APPENDIX 3

SCHEDULE

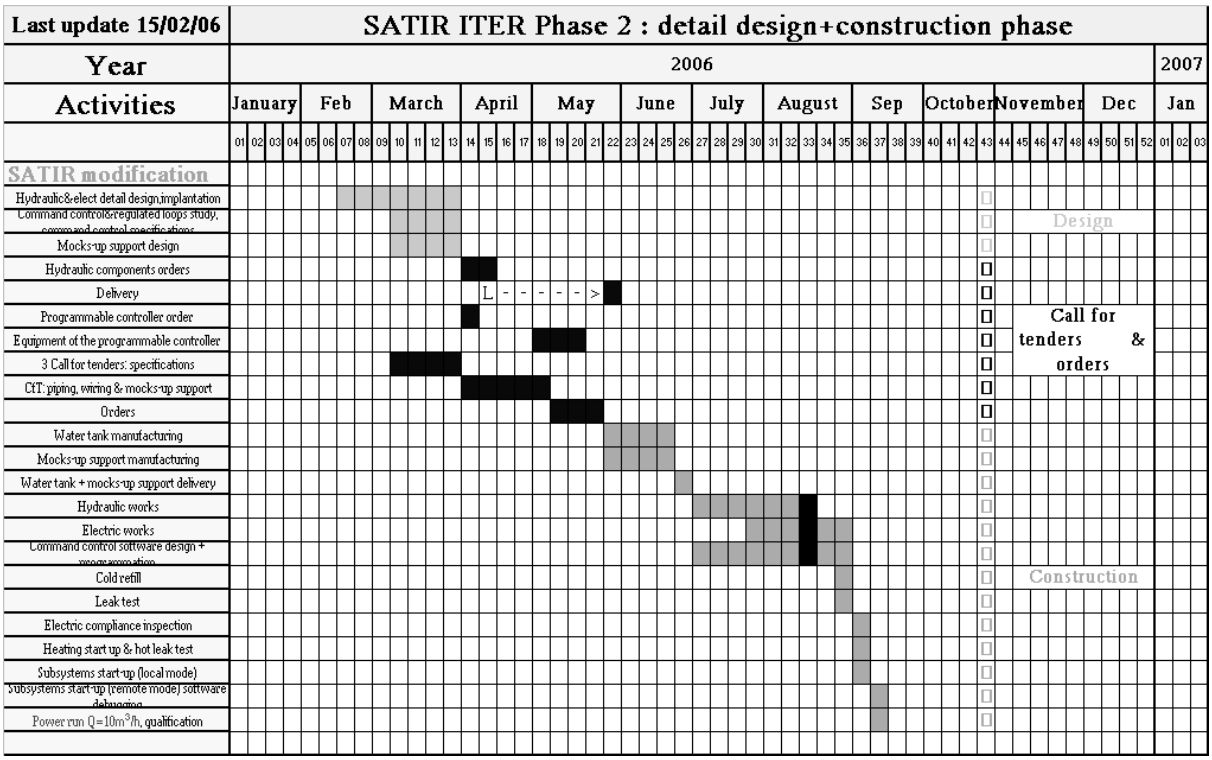

CEFDA05-1248

Task Title: TW5-TVD-ACCEPT: INFLUENCE OF CARBON EROSION ON THE ACCEPTANCE CRITERIA OF THE ITER DIVERTOR ANSYS MODEL FOR EROSION

INTRODUCTION

The whole study consists in modelling the geometrical evolution of the eroded carbon monoblocks of the ITER Divertor during normal and off-normal operations, taking into account the distribution of their properties. The related acceptance criteria for SATIR tests should be determined to ensure the lifetime of the components, given a statistical variation of material properties. The 2005 activity consists in the analysis of the erosion model developed by ITER, which calculates the heating and the erosion of sets of carbon monoblocks subject to plasma heat flux at low angles.
For the detached plasmas, the ion temperature is generally below the physical sputtering threshold for carbon, and one is left only with chemical sputtering and thermal sublimation. Above the threshold the situation is complicated by radiation enhanced sublimation and carbon self-sputtering with radiation-enhanced sublimation. Whichever case is assumed a feature of the temperature dependence is a peak of the erosion at around 900 K (see figure 1).

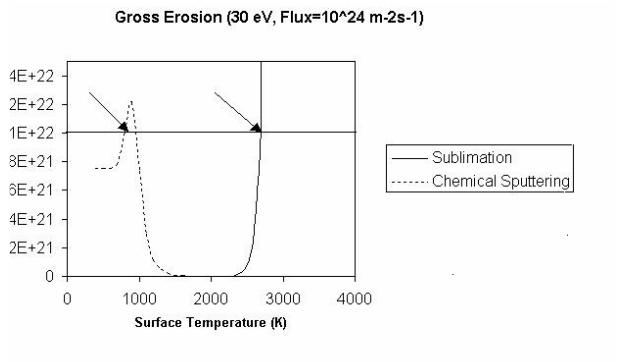

Figure 1: Gross erosion flux as function of surface temperature for detached plasma case.
The arrows show a bifurcated temperature steady state solution.

The dominant sputtering processes of graphite under hydrogen ion irradiation for different temperature ranges are summarized in table 1 (cf. [1], [2]).

Table 1: Theoretical main sputtering processes for graphite under hydrogen ion irradiation.

Temperature range (K)	Main sputtering process
0 – 500 and 900 - 1300	Physical sputtering
500 - 900	Chemical sputtering
1100 - 2000	Radiation enhanced sublimation
> 2000	Thermal sublimation

Physical sputtering occurs for all materials, independently of the chemical nature of the projectile and target atoms and of temperature. The surface atoms are ejected if they have received a sufficient kinetic energy from the incident ions to overcome the surface binding energy of the solid Es. This leads to mono-atomic carbon (C1) emission. A non-perpendicular angle of incidence enhances the sputtering yield [1].

Chemical sputtering is due to the chemical affinity between the implanted particles and the target materials. The ions penetrate at a depth of about a few hundred nanometres, diffuse in the bulk material and get trapped. Finally the hydrogen will react with carbon atoms or recombine with other implanted ions. These complex reactions lead to the emission of hydrocarbons (such as CH_4, C_2H_x, CH_3 radicals and heavier hydrocarbons) and H_2 molecules [3].

Radiation enhanced sublimation (RES) is specific to carbon-based materials having a graphitic structure. The incident ions create interstitial carbon atoms with a large mobility throughout the basal plane of the graphitic structure. Those may either recombine, agglomerate to form clusters or migrate then diffuse towards the surface and finally escape very easily (Van der Waals forces) from the material. This leads to the emission of mono-atomic carbon (C1) with an isotropic angular distribution [1].

Thermal sublimation consists essentially of the release of C1, C2 and C3 species [1]. As a phase transition it is characterized by a sudden change in physical properties, in particular the heat capacity, but a small change in a thermodynamic variable such as the temperature. When the ambient pressure equals the vapour pressure of the solid, the solid and vapour are in equilibrium. This is the equilibrium vapour pressure or saturation vapour pressure of the substance at the considered temperature. If the temperature decreases, vapour will condensate to solid; if the temperature increases, solid will turn to vapour to establish a new equilibrium condition. When the ambient pressure is ~0 Pa (in high vacuum), and kept at ~0 Pa (by pumping out the carbon ions), an equilibrium temperature is achieved, as a function of the thermal load applied onto the tile (the surface temperature is the main parameter that governs the “expulsion” of the ions from the heated surface).

Brittle destruction occurs under thermal stress. Cracks propagate and cause holes in the exposed surface with emission of debris.

This **2D ANSYS model** was developed by the ITER International Team [4] with the purpose of calculate the heating and the erosion of sets of carbon monoblocks (CFC

armour with a CuCrZr cooling tube and a pure copper compliance layer) subject to plasma heat flux at low angles (3°).

As shown on figure 2, the geometry consists in a central monoblock surrounded by two halves of one monoblock (with cyclic conditions: the temperature at the left node is coupled with the temperature at the right node). It is possible to consider the presence of a CFC/Cu bonding defect within the central monoblock. To simulate the erosion progress, a refined mesh (100 µm × 9 µm) has been used up to 2 mm under the top surface of the components. Once the input data (material properties, monoblock dimension, type of thermal analysis, heat load, thermo-hydraulic conditions, mesh size, CFC/Cu defect characteristics…) have been provided to the code (through an interactive mode or within specific files), it calculates, for each element and time step, the integral on the time of the sublimated material. If the eroded thickness is above the thickness of the element, it is killed at the next time step; the heat load is applied to the new profile and the code goes this way until the end of the simulation.

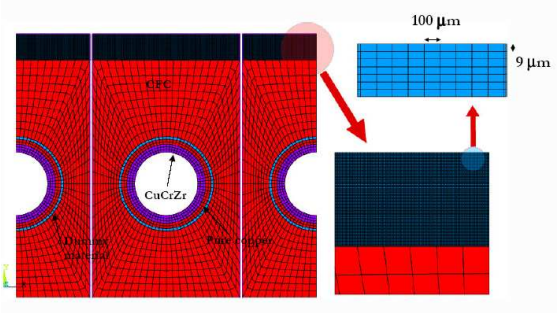

Figure 2: 2D modelling of neighbouring carbon monoblocks

CONCLUSIONS

The ANSYS 2D model for the simulation of carbon monoblocks erosion is currently developed by the ITER International Team CEA provided experimental data from the literature for a better understanding of the involved phenomena and also from ITER technology development for the forthcoming validation of the model.
So far the erosion due to the thermal sublimation has been taken into account. The chemical and physical erosion, and the possible radiation enhanced sublimation still have to be implemented. It worth being noticed that the shielding effect decreases considerably the erosion, by a factor of about 1000 for CFC; this may have to be included in the model. Enhancement of erosion by brittle destruction may be considered in case of thermal fatigue cycling.

FUTURE WORK

The model shall be achieved by implementing the various phenomena and validated on the basis of the few available experimental data. Then the study will consist in running the model for various material properties and plasma conditions reflecting those expected for ITER, in order to determine the acceptable range of thermal properties of the carbon monoblocks from the point of view of excessive erosion, the related acceptance criteria for the SATIR tests and/or optimization of the starting thickness of carbon.

REFERENCES

[1] T. Paulmier *et al.*, Physico-chemical behaviour of carbon materials under high temperature and ion irradiation, Applied Surface Science, 180 (2001), 227-245

[3] J. Roth, Chemical erosion of carbon based materials in fusion devices, Journal of Nuclear Materials, 266-269 (1999), 51-57

[4] E. D'Agata, S. Grigoriev, G. Federici, C. Ibbott, A. Makhankov, V. Tanchuk and R. Tivey, Behaviour of the PFC tiles on the ITER divertor under critical loading conditions Fusion Engineering and Design, 66-68 (2003), 329-334

REPORTS AND PUBLICATIONS

[2] CFP/NTT-2005.013, Influence of the carbon erosion on the acceptance criteria of the ITER divertor EFDA CONTRACT N°05-1248 INTERMEDIATE REPORT 1: ANSYS model for erosion simulation

TASK LEADER

Jacques SCHLOSSER

DSM/DRFC/SIPP/GCFP
CEA-Cadarache
F-13108 Saint-Paul-lez-Durance Cedex

Tel. : 33 4 42 25 25 44
Fax : 33 4 42 25 49 90

e-mail : jacques.schlosser@cea.fr

Not available on line

Not available on line

TW1-TVP-CFC1

Task Title: NEUTRON EFFECTS ON DIMENSIONAL STABILITY AND THERMAL PROPERTIES OF CFCs

INTRODUCTION

Carbon Fiber Composites (CFCs) are considered as an attractive choice for high heat flux components in existing and forthcoming tokamaks such as ITER. Two CFCs are particularly interesting for fusion devices: NB31 from SNECMA which is a 3D CFC constituted by a NOVOLTEX preform, with P55 ex-pitch fibers in the high thermal conductivity direction and NS31 which is a Si doped 3D N31 CFC [1].
In one hand, the aim of this task is to study density, specific heat capacity and thermal conductivity changes of NB31 and NS31 irradiated in the PARIDE (PlAsma facing mateRIals for ITER and DEMO) 3 and 4 irradiations, performed in HFR/Petten at 250/260°C with two damage levels (0.24 and 0.83 dpa.g) [2]. Moreover the activity of the different radionuclides contained in these two CFCs has been measured. In the other hand, the study of the dimensional, density and thermal conductivity changes of the same CFCs grades irradiated in the RBT-6 nuclear reactor (Dimitrovgrad, Russia) at 90°C with damage levels ranging from 0.002 to 0.13 dpa.g has been carried out.

2005 ACTIVITIES

In 2005, NB31 and NS31 dimensional, density and thermal conductivity measurements after irradiation in the RBT-6 reactor have been carried out [3]. Moreover, quantitative γ spectrometry results of irradiated NB31 and NS31 CFCs carried out in july 2003 are reported in order to check semi–quantitative γ spectrometry results carried out in january 2003 and reported previously [2].
The NB31 and NS31 samples were irradiated in the RBT-6 reactor at 90 ± 10°C. The fast neutron flux in the active zone is 4.1 – 6.7 10^{13} n.cm^{-2}.s^{-1} (E > 0.1 MeV). The samples have been irradiated at five different fluences (table 1).

Table 1: Fluences and neutron damages received by the irradiated samples

Fluence 10^{19} n.cm^{-2} (E > 0.1 MeV)	Damage (dpa.g)
0.28	0.0021
1.85	0.014
3.31	0.025
8.86	0.067
17.2	0.13

DIMENSIONAL CHANGES

NB31 and NS31 dimensional changes have been measured in the three directions: X direction (ex-pitch fibers direction), Y direction (ex-PAN direction) and Z direction (needling direction). For NB31, there is no significant dimensional change up to 0.067 dpa.g (figure 1); at higher neutron damage (0.13 dpa.g), there is a slight shrinkage (-0.8 %) in the ex-pitch fibers direction, a slight swelling (0.9 %) in the ex-PAN fibers direction and a swelling (3.2 %) in the needling direction. This anisotropic dimensional behaviour is expected after irradiation at so low temperature and has already been reported for a 2D Russian CFC irradiated in the same conditions [4].

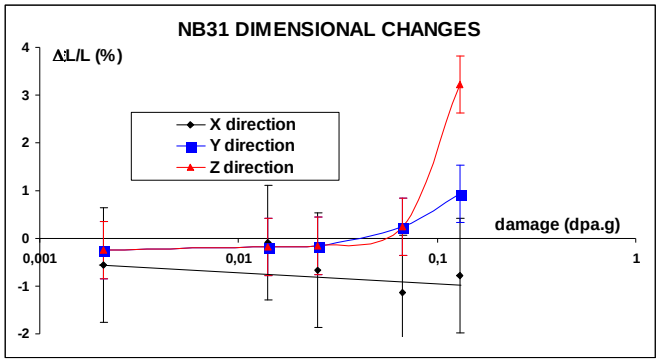

Figure 1: NB31 dimensional changes after irradiation at 90°C

For NS31, there is no significant dimensional change in the X direction up to 0.13 dpa.g. In the Y and Z directions significant dimensional changes appear beyond 0.067 dpa.g, that means, shrinkage in the ex-PAN fibers direction and swelling in the needling direction (figure 2).

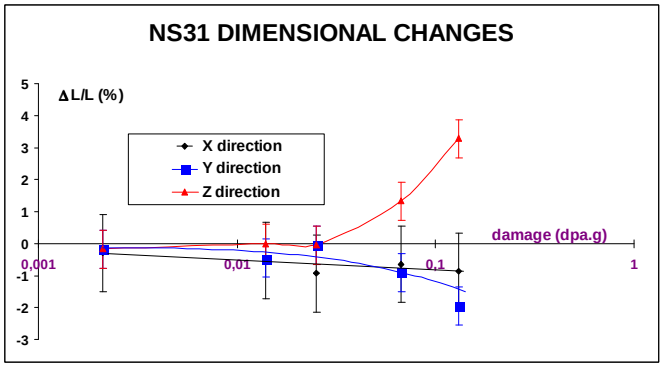

Figure 2: NS31 dimensional changes after irradiation at 90°C

DENSITY CHANGES

Up to 0.067 dpa.g, there is no significant densification (0.3 % to 1 %) of NB31, then a density loss occurs at higher damages (- 3.8 % at 0.13 dpa.g), mainly due to the swelling in the needling direction (figure 3). For NS31, there is no significant density change (-0.7 % to 0.7%) up to 0.13 dpa.g.

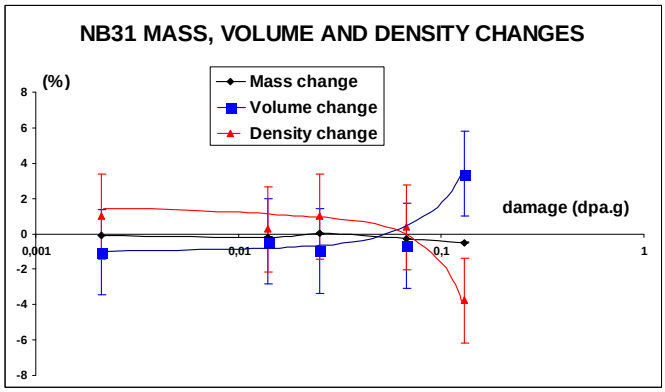

Figure 3: NB31 mass, volume and density changes after irradiation at 90°C

HEAT CAPACITY AND STORED ENERGY

The heat capacity of these CFCs has been measured before irradiation (table 2) [5]. The heat capacity values of the irradiated CFCs used for the thermal conductivity calculations are those measured in the PARIDE 3 and PARIDE 4 irradiations [2].

Table 2: NB31 and NS31 heat capacity before irradiation

Measurement temperature (K)	NB31 Cp_0 ($J.kg^{-1}.K^{-1}$)	NS31 Cp_0 ($J.kg^{-1}.K^{-1}$)
298	723	710
323	778	766
373	918	898

Stored energy often referred as Wigner energy, occurs in neutron irradiated graphite because carbon atoms are displaced by fast neutrons from their initial lattice positions into configurations of higher potential energy. During irradiation, simultaneous thermal and irradiation annealing takes place, but there is a net energy gain which depends on both neutron fluence and irradiation temperature. For graphite irradiation temperatures higher than 350°C the accumulation of stored energy is negligible. Below 350°C significant amount of Wigner energy can be accumulated, moreover at irradiation temperatures below 150°C, the amount of energy is larger and may be released at lower temperature. Graphite thermal instability due to Wigner energy occurs if the two following conditions are fulfilled:

- Irradiation temperature < 115°C
- Neutron fluence > 1.54 10^{20} $n.cm^{-2}$ (E > 0.1 MeV)

In practice, for graphite irradiated between 30°C et 120°C, most of the stored energy is concentrated in a « peak » located around 200°C. The height of this « peak » decreases when the irradiation temperature increases.

CFCs, such as NB31, are constituted of graphitic structures; therefore Wigner energy is stored in such materials when they are irradiated at low temperature.
It is possible to get a stored energy evaluation in NB31, using a comparison with graphite irradiated in G1 French gas cooled reactor at a temperature leading to the same damage level, due to neutron flux effects. Due to the difference of neutron flux in G1 (0.2 10^{13} $n.cm^{-2}.s^{-1}$) and in the RBT-6 reactor (5.4 10^{13} $n.cm^{-2}.s^{-1}$); an irradiation temperature of 90°C in the RBT-6 is equivalent to an irradiation temperature of 61°C in G1.
The enthalpy $H(\theta)_{400}$ obtained by integration between 20°C and 400°C of the energy spectrum measured by differential thermal analysis, with samples irradiated in G1 at 60 °C and 1.66 10^{20} $n.cm^{-2}$ (E > 0.1 MeV) corresponding to 0.125 dpa.g, is 326 J/g [6]. So, we can assume that the enthalpy $H(\theta)_{400}$ of NB31 irradiated at 0.13 dpa.g, is about 326 J/g.

THERMAL CONDUCTIVITY CHANGES

The NB31 thermal conductivity at 100°C before irradiation is 328 $W.m^{-1}.K^{-1}$. After irradiation at 90°C, it dramatically drops to 80 $W.m^{-1}.K^{-1}$ when the neutron damage is 0.0021 dpa.g and to 5.3 $W.m^{-1}.K^{-1}$ when the neutron damage is 0.13 dpa.g (figure 4). The NS31 thermal conductivity shows exactly the same behaviour after irradiation in the same conditions. These results are in very good agreement with those provided by Barabash et. al [7].

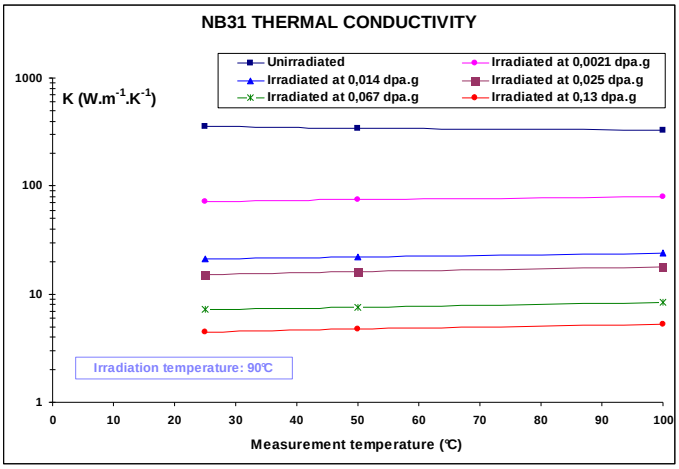

Figure 4: NB31 thermal conductivity as a function of the measurement temperature for different neutron damages

Generally, CFC normalized thermal conductivity at the irradiation temperature $(K_i/K_0)_{Tirr}$ decreases with increasing neutron damage for irradiation temperature between 400°C and 1200°C. This decrease is a logarithmic function of neutron damage from 10^{-3} to 2 dpa.g. However this is not the case for NB31 and NS31 $(K_i/K_0)_{Tirr}$ after irradiation at 90°C. This ratio strongly decreases at the lower neutron damage, then this decrease becomes smaller and smaller as the neutron damage increases, to finally reach a saturation level (figure 5).
The irradiation temperature is the main parameter in the thermal conductivity changes. After irradiation at very low damage (~ 0.1 dpa.g), CFCs $(K_i/K_0)_{Tirr}$ ratio increases of a factor 8 when the irradiation temperature increases from 90°C to 150°C, and of a factor 21 when it increases from 90°C to 400°C.

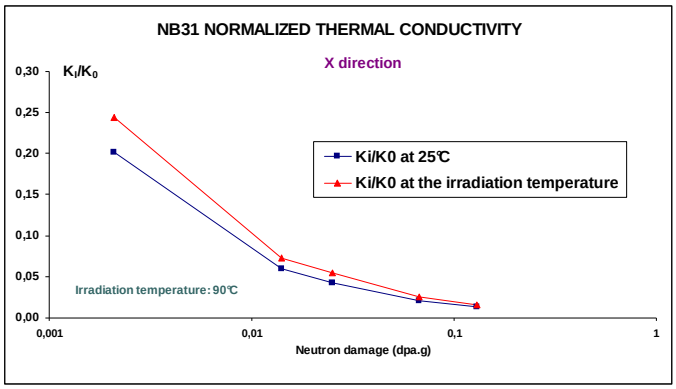

Figure 5: NB31 thermal conductivities as a function of neutron damage after irradiation at 90°C

γ SPECROMETRY OF CARBON FIBER COMPOSITES IRRADIATED IN PARIDE 3 AND 4 IRRADIATIONS

In july 2003, quantitative γ spectrometry measurements have been carried out on NB31 (tables 3 and 4) and NS31 (table 5) samples irradiated in PARIDE 3 and PARIDE 4 irradiations (HFR/Petten), in order to check the activity values of semi-quantitative measurements performed in December 2002 on the same NB31 (tables 6 and 7) and NS31 (table 8) samples.

Table 3: γactivity in december 2002 (Bq/g), measured in july 2003, of NB31 irradiated at 260°C/0.24 dpa.g

Isotope	γ activity (Bq/g)	Distribution of the γ activity (%)
Total	**2460**	**100**
^{60}Co	1150	46.7
^{152}Eu	840	34.1
^{154}Eu	290	11.8
^{155}Eu	90	3.7
^{46}Sc	20	0.8
^{54}Mn	60	2.4
^{65}Zn	10	0.4

Table 4: γactivity in december 2002 (Bq/g), measured in july 2003, of NB31 irradiated at 250°C/0.83 dpa.g

Isotope	γ activity (Bq/g)	Distribution of the γ activity (%)
Total	**6330**	**100**
^{60}Co	3430	54.2
^{152}Eu	520	8.2
^{154}Eu	1580	25
^{155}Eu	630	10
^{46}Sc	30	0.5
^{54}Mn	120	1.9
^{65}Zn	20	0.3

Table 5: γactivity in december 2002 (Bq/g), measured in july 2003, of NS31 irradiated at 250°C/0.83 dpa.g

Isotope	γ activity (Bq/g)	Distribution of the γ activity (%)
Total	**155260**	**100**
^{60}Co	131260	83.9
^{152}Eu	2420	1.5
^{154}Eu	2770	1.7
^{155}Eu	1040	0.5
^{46}Sc	440	0.1
^{54}Mn	16020	11.7
^{65}Zn	1310	0.6

Table 6: γactivity in december 2002 (Bq/g), measured in december 2002, of NB31 irradiated at 260°C/0.24 dpa.g

Isotope	γ activity (Bq/g)	Distribution of the γ activity (%)
Total	**4250**	**100**
^{60}Co	2000	47.1
^{152}Eu	1400	32.9
^{154}Eu	510	12
^{155}Eu	170	4
^{46}Sc	40	0.9
^{54}Mn	100	2.4
^{65}Zn	30	0.7

Table 7: γactivity in december 2002 (Bq/g), measured in december 2002, of NB31 irradiated at 250°C/0.83 dpa.g

Isotope	γ activity (Bq/g)	Distribution of the γ activity (%)
Total	**11350**	**100**
^{60}Co	5970	52.6
^{152}Eu	910	8
^{154}Eu	2720	24
^{155}Eu	1400	12.3
^{46}Sc	60	0.5
^{54}Mn	220	1.9
^{65}Zn	70	0.6

Table 8: γactivity in december 2002 (Bq/g), measured in december 2002, of NS31 irradiated at 250°C/0.83 dpa.g

Isotope	γ activity (Bq/g)	Distribution of the γ activity (%)
Total	**276000**	**100**
^{60}Co	231520	83.9
^{152}Eu	4100	1.5
^{154}Eu	4770	1.7
^{155}Eu	1480	0.5
^{46}Sc	250	0.1
^{54}Mn	32250	11.7
^{65}Zn	1630	0.6

The γ activities as given by quantitative γ spectrometry measurements are 43 % lower than those as given by the semi-quantitative method. For NB31, the ratio of the activity after irradiation at 0.83 dpa.g on that after irradiation at 0.24 dpa.g, is in good agreement with the ratio of the fluences. Half of the irradiated NB31 total γ activity is provided by ^{60}Co. In the same irradiation conditions, the NS31 total γ activity is 24 times larger than that of NB31. More than 80 % of the NS31 total activity is due to ^{60}Co, mainly produced by the reaction ^{59}Co (n,γ) ^{60}Co. This means that NS31 contains a larger cobalt impurity amount than NB31.

CONCLUSIONS

The main conclusions which can be drawn from these irradiation experiments are the following:

- For NB31 and NS31, significant dimensional changes appear beyond 0.067 dpa.g. For NB31, there is a slight shrinkage in the ex-pitch fibers direction, a slight swelling in the ex-PAN fibers direction and a larger swelling in the needling direction. For NS31, there is a shrinkage in the ex-PAN fibers direction and a swelling in the needling direction.

- NB31 shows a density loss at 0.13 dpa.g, mainly due to the swelling in the needling direction. For NS31, there is no significant density change.

- During irradiation at 350°C, significant amount of Wigner energy can be stored in CFCs. Using a comparison with graphite irradiated in G1 reactor, we have made the assumption that the $H(\theta)_{400}$ of NB31 irradiated at 90°C/0.13 dpa.g is about 326 J/g.

- After irradiation at 90°C, the NB31 and NS31 thermal conductivity dramatically drops even at neutron damage as low as 0.13 dpa.g.

- Generally, CFC normalized thermal conductivity $(K_i/K_0)_{Tirr}$ shows a decrease with increasing neutron damage from 10^{-3} to 2 dpa.g, for irradiation temperature ranging from 400°C to 1200°C. However this is not the case for NB31 and NS31 $(K_i/K_0)_{Tirr}$ after irradiation at 90°C.

- The irradiation temperature is the main parameter in the thermal conductivity changes. After irradiation at 0.1 dpa.g, CFCs $(K_i/K_0)_{Tirr}$ ratio increases of a factor 8 when the irradiation temperature increases from 90°C to 150°C.

- The γ activities as given by quantitative γ spectrometry measurements are 43 % lower than those as given by the semi-quantitative method. Half of the NB31 and 80 % of the NS31 total γ activities are provided by ^{60}Co. In the same irradiation conditions, the NS31 total γ activity is 24 times larger than that of NB31.

REFERENCES

[1] Simulation experimental investigation of plasma off-normal events on advanced silicon doped CFC-NS31 - J.P. BONAL, C.H. WU, D. GOSSET
Journal of Nuclear Materials 307-311 (2002) p. 100-105.

[4] Post-irradiation strength of carbon candidate constructional materials for fusion reactors" O.I. BUZHINSKIJ, YU.S. VIRGILIEV, E.I. KUROLENKIN
Journal of Nuclear Materials 185 (1991) 78-86

[6] Energie emmagasinée par le graphite irradié. Effet de la température d'irradiation" - J. RAPPENEAU
Journal of Nuclear Materials 6, N°1 (1962), p 107-118

[7] The effect of low temperature neutron irradiation and annealing on the thermal conductivity of advanced carbon-based materials
V. BARABASH, I. MAZUL, R. LATYPOV, A. POKROVSKY, C.H. WU
Journal of Nuclear Materials 307-311 (2002) 1300-1304

REPORTS AND PUBLICATIONS

[2] Thermal properties changes of carbon fiber composites irradiated at low temperature. PARIDE 3/4 experiment - J.P. BONAL
Rapport DMN/SEMI/LM2E/RT/03-009/A

[3] Neutron irradiation effects on NB31 and NS31 carbon fiber composites irradiated at low temperature. - J.P. BONAL
Document technique DMN/SEMI/LM2E/RT/03-009/A

[5] Thermal properties of carbon fiber composites before irradiation in PARIDE 3/4 experiment" J.P. BONAL
Rapport DMT SEMI/LM2E/RT2004, janvier 2000

TASK LEADER

Jean-Pierre BONAL

DEN/DMN/SEMI/LM2E
CEA-Saclay
F-91191 Gif-sur-Yvette Cedex

Tel. : 33 1 69 08 50 58
Fax : 33 1 69 08 90 73

e-mail : jean-pierre.bonal@cea.fr

Not available on line

Not available on line

Not available on line

Not available on line